ISSN 0030-400X, Optics and Spectroscopy, 2021, Vol. 129, No. 6, pp. 824–828. © Pleiades Publishing, Ltd., 2021.
Russian Text © The Author(s), 2021, published in Optika i Spektroskopiya, 2021, Vol. 129, No. 6, pp. 736–740.

BIOPHOTONICS

# Study of the Photocatalytic Antimicrobial Activity of Nanocomposites Based on $TiO_2$–$Al_2O_3$ under Action of LED radiation (405 nm) on Staphylococci

**A. V. Svetlakova[a, *], M. Sanchez Mendez[c], E. S. Tuchina[a], A. N. Khodan[b], M. Traore[c], R. Azouani[d], A. Kanaev[c], and V. V. Tuchin[a, e, f]**

[a] *Chernyshevsky Saratov State University, Saratov, 410012 Russia*
[b] *Frumkin Institute of Physical Chemistry and Electrochemistry, Russian Academy of Sciences, Moscow, 119071 Russia*
[c] *Laboratoire des Sciences des Procédés et des Matériaux, CNRS, Université Sorbonne Paris 8 Nord, F-93430, Villetaneuse, France*
[d] *EBInnov, École de Biologie Industrielle, F-95000, Cergy, France*
[e] *National Research Tomsk State University, Tomsk, 634050 Russia*
[f] *Institute for Problems of Precision Mechanics and Control, Russian Academy of Sciences, Saratov, 410028 Russia*
**e-mail: anna5vetlakova@yandex.ru*

Received January 11, 2021; revised January 29, 2021; accepted February 26, 2021

**Abstract**—We study the photocatalytic activity of nanocomposites based on θ-phase alumina ($Al_2O_3$) with different $TiO_2$ concentrations for heterogeneous photocatalysis and biodestruction of pathogenic microorganisms under action of LED radiation with a wavelength of 405 nm. It is found that all studied nanocomposites have photocatalytic activity. The maximum antibacterial activity (a decrease in the CFU of *Staphylococcus aureus* 209 P to 86%) is observed for composites with a $TiO_2$ concentration of 8 wt %, which allows us to recommend this nanomaterial as a promising antimicrobial coating.

**Keywords:** photocatalytic action, θ-$Al_2O_3$, $TiO_2$, 405-nm LED radiation, antibacterial efficiency, *Staphylococcus aureus* 209 P

**DOI:** 10.1134/S0030400X21060175

## INTRODUCTION

As is admitted by the world medical community, the unnecessary use of antibiotics, which was enormous during the COVID-9 pandemic, may have a long-term complex effect on the resistance of infectious bacterial agents to antimicrobial drugs [1]. The effect of various modern nanomaterials is based on fundamentally different antibacterial mechanisms and thus do not allow bacterial cells to form resistivity to these materials [2].

Among these mechanisms are photodynamic or photocatalytic antimicrobial effects [3–9]. The photodynamic antibacterial effect is based on the ability of various endogenic or exogenic dyes (photosensitizers) to produce in an irradiated biological medium free radicals (reactive oxygen species (ROSs)), which cause peroxidation of lipids, destruction of membranes, and distortion of the DNA structure and organelles of microorganisms [3, 4]. The photocatalytic antimicrobial mechanism is associated with the transition of a valence electron under light irradiation to the conduction band of the photocatalytic material, which also leads to the formation of ROSs, mainly hydroxyl radicals (·OH), which play the role of holes in aqueous media and cause oxidation of biological molecules [5–10]. Photocatalysis with the use of oxide metals is more and more frequently used in antibacterial therapy, because of which the search for new promising nanocomposites (NCs) is an actual problem of modern science.

Aluminum oxide exists in several modifications, the most widespread being α-, γ-, and θ-modifications, which differ from each other in density and band gap width [11–19]. The θ-phase is most frequently used in photocatalysis [7, 11, 13], while the properties and photocatalytic efficiency of the other $Al_2O_3$ phases are studied insufficiently. In contrast, $TiO_2$ is used in many industrial fields and in medicine, and its photocatalytic properties are rather well studied [10, 20–28]. Comparison of the antibacterial activity of pure θ-$Al_2O_3$ and NCs with different concentrations of nanodispersed $TiO_2$ will make it possible to determine the optimal composition and morphology of composites for their application.

## MATERIALS AND METHODS

### *Nanocomposites*

$TiO_2$–$Al_2O_3$ composites with average concentrations of single $TiO_2$ nanoparticles of 8 (NC-1), 16 (NC-2), and 24 wt % (NC-3) were fabricated by the method described previously in [29, 30]. At the first stage, the initial samples of highly porous 3D monolithic nanostructures consisting of aluminum oxyhydroxide ($Al_2O_3 \cdot 3.6H_2O$) were grown at room temperature in a humid atmosphere by oxidation of aluminum on the surface of a liquid mercury layer on high-purity metal aluminum plates. Then, all samples obtained were thermally treated in air at 1150°C for 4 h to achieve the desired structural-phase state—θ-$Al_2O_3$ [31, 32]. At the second stage, $TiO_2$–$Al_2O_3$ nanocomposites were formed. For this purpose, we used a sol–gel reactor with an ultrafast micromixer at 20°C to synthesize titanium oxoalkoxide nanoparticles with a size of 5.2 ± 0.5 nm. The reactive medium contained titanium tetraisopropoxide with $C_{Ti}$ = 0.146 M and water with a hydrolysis ratio $H = C_W/C_{Ti} = 2.2$. The photocatalysts were obtained by repetitive cycles of impregnation/drying of 3D matrices of θ-$Al_2O_3$, which allowed us to control the total weight of sediment $TiO_2$ nanoparticles. At the final stage, NCs were thermally treated at 550°C for 4 h for crystallization of $TiO_2$ anatase domains. We have previously shown that single $TiO_2$ nanoparticles 5 nm in size deposited on an aluminum oxide surface begin to crystallize in the anatase phase at a temperature increased to 550°C, while the rutile phase appears only at temperatures of about 1100°C [33]. The presence of some amount of amorphous $TiO_2$ nanoparticles in the samples cannot be excluded. It is noted that strong covalent bonds are formed at the impregnation stage between hydroxylated titania and alumina centers. According to our previous results [29, 30], the specific material area (115 $m^2/g$) does not depend on the degree of impregnation by nanoparticles. The weight of sediment $TiO_2$ nanoparticles was measured by the method of ammonium sulfate ($NH_4SO_4$) decomposition into $H_2SO_4$; for comparison, we used a θ-$Al_2O_3$ sample without impregnation by titanium oxide.

### *Bacterial Culture and Photoirradiation Technique*

We studied an archival *S. aureus* 209 P strain from the collections of the Tarasevich State Institute of Standardization and Control of Biomedical Preparations (Moscow, Russia). We used 24-h cultures grown on the universal nutrient medium GRM-agar (Obolensk, Russia).

As a radiation source, we used an experimental setup based on a cw light-emitting diode (LED) with a wavelength of 405 nm and a line halfwidth of 10 nm. The power density on the object was 17 mW/$cm^2$, and the exposure times were 5, 10, 15, and 30 min (irradiation energy density was 5.1, 10.2, 15.3, and 30.6 J/$cm^2$, respectively).

The experimental scheme, which was previously described in [19], was adapted to work with NCs. A bacterial suspension 1 mL in volume was added into a polystyrene plate well with an average diameter of 10 mm containing the studied materials in the form of plates 8 mm in diameter and 2 mm thick. The obtained mixture was kept in dark for 30 min. Then, the suspension was irradiated during 5, 10, 15, or 30 min. After irradiation, the culture with a volume of 0.2 ml was poured into Petri dishes with a dense nutrient medium.

The results were estimated by calculating the number of colony forming units (CFU) 24–48 h after incubation at 37°C. As a reference, we used the colony-forming ability of unirradiated bacteria in the absence of NCs.

## RESULTS AND DISCUSSION

At the first stage, we estimated the toxicity of NCs in dark depending on the incubation duration (Fig. 1). It is found that the interaction of $Al_2O_3$ samples without $TiO_2$ with bacterial cells during 30–120 min leads to an insignificant (no more than 17%) decrease in the number of CFUs. Incubation of the *S. aureus* 209 P suspension in the presence of this sample prolonged to 150 min caused a slightly more pronounced decrease (to 34%) in the number of these microorganisms.

A similar dynamics of the bacteria population was observed for samples containing 8 and 24 wt % of $TiO_2$. The most pronounced toxic effect on *S. aureus* 209 P was demonstrated by the NC sample containing 16 wt % of $TiO_2$, namely, we observed a 58% decrease in the number of CFUs in the case of incubation for 30 min and a 84% decrease in the case of incubation for 180 min.

For proper estimation of the photocatalytic activity of NCs, it was necessary to determine the sensitivity of the microorganisms under study to the 405-nm LED radiation alone. It was shown that a decrease in the number of *S. aureus* 209 P bacteria is 25% after 15-min irradiation and 31% after irradiation for 30 min. The sensitivity of the bacterial structure to the action of the LED radiation at 405 nm is explained by the fact that staphylococcus cells contain endogenous porphyrins [3, 34, 35], which have the absorption maximum in the violet range of the visible spectrum (400–415 nm). Violet radiation with a power density of about 100 mW/$cm^2$ exerts a bactericidal effect [35], while radiation with a power density of 30–70 mW/$cm^2$ suppresses the population of bacteria by no more than 30%, which was also noted in our previous works [20, 21, 28]. The use of a decreased radiation power density makes it possible to selectively affect target cells related to NCs by activating photocatalytic processes

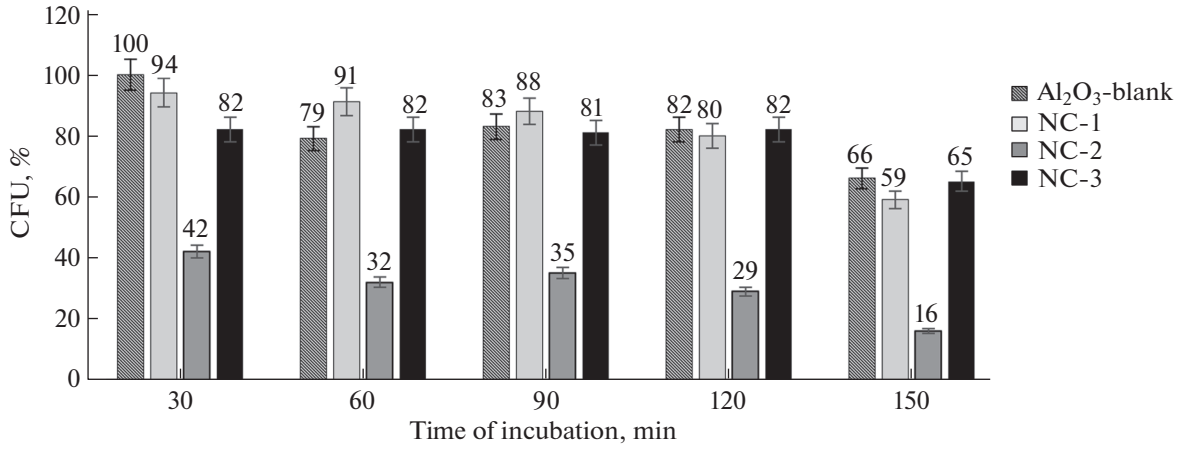


**Fig. 1.** Change in the amount of CFUs of *S. aureus* 209 P in the presence of $Al_2O_3$ nanocomposites with increasing incubation duration: ($Al_2O_3$-blank) θ-$Al_2O_3$ nanocomposites; (NC-1) nanocomposites containing θ-$Al_2O_3$ and 8 wt % of $TiO_2$ nanoparticles; (NC-2) nanocomposites containing θ-$Al_2O_3$ and 16 wt % of $TiO_2$ nanoparticles; and (NC-3) nanocomposites containing θ-$Al_2O_3$ and 24 wt % of $TiO_2$ nanoparticles.

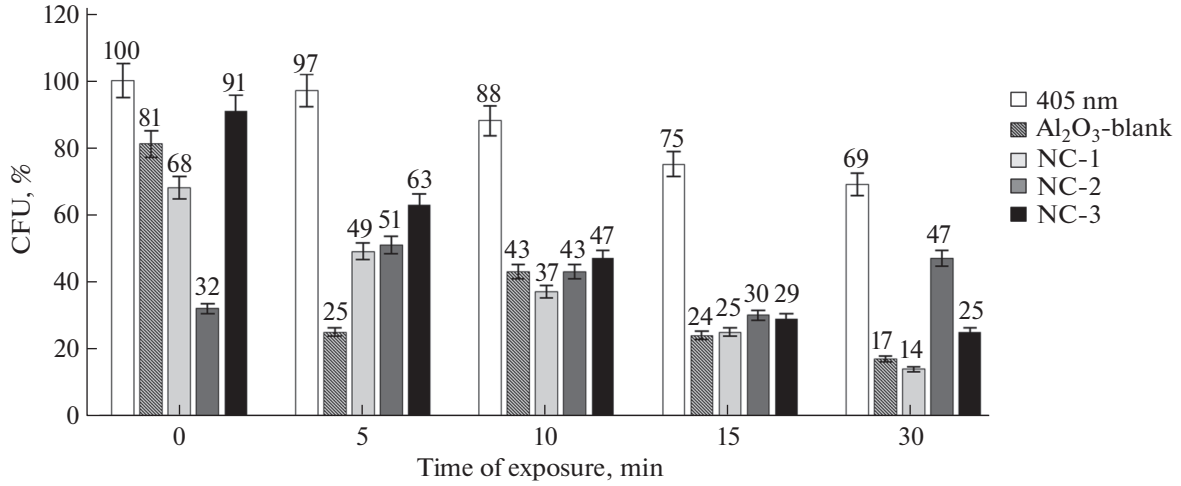


**Fig. 2.** Change in the amount (%) CFUs of *S. aureus* 209 P due to photocatalytic activity of $Al_2O_3$ nanocomposites: (405 nm) irradiation by a violet LED; ($Al_2O_3$-blank) violet radiation and nanocomposites containing θ-$Al_2O_3$; (NC-1) violet LED radiation and nanocomposites containing θ-$Al_2O_3$ and 8 wt % of $TiO_2$ nanoparticles; (NC-2) violet radiation and nanocomposites containing θ-$Al_2O_3$ and 16 wt % of $TiO_2$ nanoparticles; and (NC-3) violet LED radiation and nanocomposites containing θ-$Al_2O_3$ and 24 wt % of $TiO_2$ nanoparticles.

without considerable direct destructive effect on microorganisms.

In the course of investigation of the photocatalytic properties of the NCs, it was found that they have a high antibacterial activity with respect to *S. aureus* 209 P (Fig. 2).

The photocatalytic activity of our samples also depended on the presence of $TiO_2$. Irradiation for 30 min together with the action of $Al_2O_3$ NCs without $TiO_2$ caused a decrease in the number of bacteria by 83%, while the suppression of the bacterial growth in the presence of $TiO_2$ with concentrations of 16 and 24 wt % reached 53% and 75%. The most intense suppression of the growth of bacterial populations (by 86%) was achieved for the NC sample containing 8 wt % of $TiO_2$. In all cases, the decrease in the number of *S. aureus* 209 P CFUs was dependent on the radiation dose.

Despite the fact that the photocatalytic properties of $Al_2O_3$ are poorly studied, it is known that this material has some advantages over other metal oxides. Pure $Al_2O_3$ has a low cytotoxicity compared to such materi-

als as $CeO_2$, $TiO_2$, and ZnO. In particular, comparison of the dark toxicity to human cells revealed that ZnO is most toxic, while $Al_2O_3$ turned out to be nontoxic even in the case of long-term action [11]. However, study of $Al_2O_3$/ZnO NCs [12] showed that they have a higher toxicity than each individual material [12].

Investigations show that pure $Al_2O_3$ nanoparticles also have a low photocatalytic activity upon irradiation. Namely, it was shown for seven strains of microorganisms that $Al_2O_3$ had the lowest antibacterial activity among the studied $Al_2O_3$, CuO, $Fe_3O_4$, and ZnO nanoparticles [13].

To increase the photocatalytic activity, $Al_2O_3$ are doped with other materials, which makes it possible to achieve the optimal band gap and minimize the loss due to the recombination of photoinduced charges. The $Al_2O_3/TiO_2$ composites belong to the most active photocatalysts. Although the optimal ratio of these oxides has not yet been determined, many investigations clearly prove an increase in the photocatalytic activity [14, 29, 30]. For example, study of the antimicrobial photocatalytic activity of $Al_2O_3/TiO_2$ composites revealed biodestruction of *Escherichia coli* microorganisms and a higher production of ROSs [15] in comparison with individual components. Apart from titanium dioxide, $Al_2O_3$ is doped with other elements, such as silver, nickel, silicon, and nitrogen. Antimicrobial photocatalytic action of these materials on some enteropathogenic bacteria and viruses was shown in several works [16–19].

Our study showed that $\theta$-$Al_2O_3$ is promising as a photocatalytic antibacterial material. Pure $Al_2O_3$ NCs demonstrated a rather low dark toxicity and a sufficiently high photocatalytic activity, which makes them applicable for targeted destruction of microorganisms under action of light.

It was shown in some studies that doping of $TiO_2$ nanoparticles with various metals and metal oxides, as well as doping of nanomaterials with hydrogen or nitrogen, shifts their absorption spectrum to the visible region [21, 22, 36–38]. This allows activation of photocatalytic processes not by UV radiation, which negatively affects all living cells, but by radiation with a wavelength in the range of 390–470 nm, which selectively affects only the "bacterial cell–nanoparticle" system.

Other factors contributing to the catalytic ability of nanoparticles are their size, band gap width, and light diffusion in the material [38–40]. In our study, the highest photoactivity was demonstrated by composites with the lowest concentration of $TiO_2$ nanoparticles (8 wt %). The presence of 5-nm anatase $TiO_2$ nanoparticles in a dense branched network of ~140-nm $Al_2O_3$ wires may increase the total reactivity of the material due to light scattering. We may suggest that the mentioned concentration of $TiO_2$ nanoparticles is favorable for this process. In addition, an excess concentration of $TiO_2$ nanoparticles also can lead to quenching of generated radicals (ROSs) [10].

Comparing the data obtained with the results of previous studies [28, 29], we can assert that the smaller size of $TiO_2$ nanoparticles (5 nm versus 25–100 nm) is responsible for more pronounced suppressive action on staphylococcus cells. It is also necessary to note that sintering of $TiO_2$ nanoparticles at temperatures exceeding 900°C (in the case of our NCs, up to 1115°C) decreases the band gap from 3.43 to 3.14 eV [38], which enhances the photocatalytic properties of materials for visible radiation.

The data obtained are of scientific and practical interest because they open the possibility of using violet LEDs for controlled suppression of bacterial populations; the photocatalytic activity of created NCs depends on some parameters and characteristics of their nanoparticles, which makes it possible to control the photocatalytic properties of NCs.

## FUNDING

The work by V.V. Tuchin was supported by the grant of the Government of the Russian Federation for state support of scientific research conducted under the supervision of leading scientists (grant no. 2020-220-08-2389).

## CONFLICT OF INTEREST

The authors declare that they have no conflict of interest.

## REFERENCES

1. T. M. Rawson, D. Ming, R. Ahmad, L. S. Moore, H. Alison, and A. H. Holmes, Nat Rev. Microbiol. **18**, 409 (2020). https://doi.org/10.1038/s41579-020-0395-y
2. W. Gao and L. Zhang, Nat. Rev. Microbiol. **19**, 5 (2021). https://doi.org/10.1038/s41579-020-00469-5
3. M. R. Hamblin, Curr. Opin. Microbiol. **33**, 67 (2016). https://doi.org/10.1016/j.mib.2016.06.008
4. G. Wei, G. Yang, Y. Wang, H. Jiang, Y. Fu, G. Yue, and R. Ju, Theranostics **10**, 12241 (2020). https://doi.org/10.7150/thno.52729
5. Z. Jia, V. Nadtochenko, M. A. Radzig, I. A. Khmel, G. Zavilgelsky, R. Azouani, and A. Kanaev, Mech. Ind. **17**, 1 (2016). https://doi.org/10.1051/meca/2015108
6. L. Wang, C. Hu, and L. Shao, Int. J. Nanomed. **12**, 1227 (2017). https://doi.org/10.2147/IJN.S121956
7. P. Ganguly, C. Byrne, A. Breen, and S. C. Pillai, Appl. Catal. B **225**, 51 (2018). https://doi.org/10.1016/j.apcatb.2017.11.018
8. C. Regmi, B. Joshi, S. K. Ray, G. Gyawali, and R. P. Pandey, Front. Chem. **6**, 1 (2018). https://doi.org/10.3389/fchem.2018.00033

9. V. N. Lad and Z. V. P. Murthy, Handbook Smart Photocatal. Mater. **1**, 3 (2020). https://doi.org/10.1016/B978-0-12-819051-7.00001-4
10. Y. Nosaka and A. Y. Nosaka, Chem. Rev. **117**, 11302 (2017). https://doi.org/10.1021/acs.chemrev.7b00161
11. I.-S. Kim, M. Baek, and S.-J. Choi, J. Nanosci. Nanotechnol. **10**, 3453 (2010). https://doi.org/10.1166/jnn.2010.2340
12. F. Li, Y. Zhao, Y. Hao, X. Wang, R. Liu, D. Zhao, and D. Chen, J. Hazard. Mater. **239**, 7058 (2010). https://doi.org/10.1016/j.jhazmat.2012.08.016
13. M. A. Ansari, H. M. Khan, M. A. Alzohairy, M. Jalal, S. G. Ali, R. Pal, and J. Mussarat, World J. Microbiol. Biotechnol. **31**, 153 (2014). doi 757-2 https://doi.org/10.1007/s11274-014-1
14. B. Li, H. Yuan, B. Yi, and Y. Zhang, Ceram. Int. **42**, 17405 (2016). https://doi.org/10.1016/j.ceramint.2016.08.040
15. R. Sikora, A. Adrian Augustyniak, K. Cendrowski, P. Nawrotek, and E. Mijowska, Nanomaterials **8**, 212 (2018). https://doi.org/10.3390/nano8040212
16. L. Jie, L. Changcheng, M. Aizeng, D. Zhijian, and Z. Huidong, China Pet. Process. Petrochem. Technol. **20**, 1 (2018).
17. S. Parham, D. Wicaksono, and Y. Nur, J. Textile Inst. **110**, 791 (2018). https://doi.org/10.3390/ma13092153
18. A. S. Lozhkomoev, S. O. Kazantsev, V. Pervikov, N. Fomenko, and I. Gotman, Mater. Res. Bull. **119**, 1105545 (2019). https://doi.org/10.1016/j.materresbull.2019.110545
19. J. S. Köerich, D. J. Nogueira, V. P. Vaz, C. Simioni, M. L. N. da Silva, L. C. Ouriques, D. S. Vicentini, and W. G. Matias, J. Toxicol. Environ. Health, Part A **83**, 363 (2020). https://doi.org/10.1080/15287394.2020.1761496
20. E. S. Tuchina and V. V. Tuchin, Laser Phys. Lett. **7**, 607 (2010). https://doi.org/10.1002/lapl.201010030
21. A. Sarkar, A. Shchukarev, A.-R. Leino, K. Kordas, J.-P. Mikkola, P. O. Petrov, E. S. Tuchina, A. P. Popov, M. E. Darvin, M. Meinke, J. Lademann, and V. V. Tuchin, Nanotechnology **23**, 475711 (2012). https://doi.org/10.1088/0957-4484/23/47/475711
22. M. Mohl, A. Dombovari, E. S. Tuchina, P. O. Petrov, O. A. Bibikova, I. Skovorodkin, A. P. Popov, A.-R. Rautio, A. Sarkar, J.-P. Mikkola, M. Huuhtanen, S. Vainio, R. L. Keiski, A. Prilepsky, A. Kukovecz, et al., J. Mater. Chem. B **2**, 1307 (2014).
23. P. V. Laxma Reddy, B. Kavitha, P. A. Kumar Reddy, and K. H. Kim, Environ. Res. **154**, 296 (2017). https://doi.org/10.1016/j.envres.2017.01.018
24. Z. Shayegan, C.-S. Lee, and F. Haghighat, Chem. Eng. J. **334**, 2408 (2018). https://doi.org/10.1016/j.cej.2017.09.153
25. B. E. Nagay, C. Dini, J. M. Cordeiro, A. P. Ricomini-Filho, E. D. de Avila, E. C. Rangel, N. C. da Cruz, and V. A. Barão, Appl. Mater. Interfaces **11**, 18186 (2019). https://doi.org/10.1021/acsami.9b03311
26. M. Bilal, B. Ambreen, J. Ali, S. Hassan, and A. U. Khan, Chem. Chem. Eng. **38**, 261 (2019).
27. A. M. Rahmati, S. F. Shayesteh, and H. F. Shayesteh, Phys. Solid State **62**, 120 (2020). https://doi.org/10.1134/S1063783420010023
28. E. S. Tuchina, M. V. Korchenova, A. V. Svetlakova, K. Kordas, and V. V. Tuchin, Izv. Sarat. Univ., Nov. Ser., Ser.: Khim. Biol. Ekol. **20**, 324 (2020).
29. M. Bouslama, M. C. Amamra, S. Tieng, O. Brinza, K. Chhor, M. Abderrabba, J.-L. Vignes, and A. Kanaev, Appl. Catal. A **402**, 156 (2011). https://doi.org/10.1016/j.apcata.2011.05.042
30. M. Bouslama, M. C. Amamra, Z. Jia, M. B. Amar, O. Brinza, K. Chhor, M. Abderrabba, J.-L. Vignes, and A. Kanaev, ACS Catal. **2**, 1884 (2012). https://doi.org/10.1021/cs300033y
31. J.-L. Vignes, C. Frappar, T. di Costanzo, J.-C. Rouchaud, L. Mazerolles, and D. Michel, Mater. Sci. **43**, 1234 (2008). https://doi.org/10.1007/s10853-007-2260-z
32. A. Khodan, T. H. N. Nguyen, M. Esaulkov, M. R. Kisele, M. Amamra, J.-L. Vignes, and A. Kanaev, J. Nanopart. Res. **20**, 194 (2020). https://doi.org/10.1007/s11051-018-4285-4
33. O. Khatim, M. Amamra, K. Chhor, T. Bell, D. Novikov, D. Vrel, and A. Kanaev, Chem. Phys. Lett. **558**, 53 (2013). https://doi.org/10.1016/j.cplett.2012.12.019
34. M. Maclean, S. J. MacGregor, J. G. Anderson, and G. A. Woolsey, J. Photochem. Photobiol. B **92**, 180 (2008). https://doi.org/10.1016/j.jphotobiol.2008.06.006
35. R. M. Tomb, M. Maclean, and J. E. Coia, Antimicrob. Resist. Infect. Control. **6**, 100 (2017). https://doi.org/10.1186/s13756-017-0261-5
36. A. V. Vorontsov and S. V. Tsybulya, Chem. Res. **57**, 2526 (2018). https://doi.org/10.1021/acs.iecr.7b04480
37. S. K. Evstropiev, N. V. Nikonorov, V. M. Kiselev, A. S. Saratovskii, and E. V. Kolobkova, Opt. Spectrosc. **127**, 314 (2019).
38. E. V. Seliverstova, N. Kh. Ibraev, and A. Zh. Zhumabekov, Opt. Spectrosc. **128**, 1449 (2020).
39. S. Kumar, N. K. Verma, and M. L. Singla, Digest J. Nanomater. Biostruct. **7**, 607 (2012).
40. K. C. Ko, S. Bromley, J. Lee, and F. Illas, J. Phys. Chem. Lett. **8**, 5593 (2017). https://doi.org/10.1021/acs.jpclett.7b02474


*Translated by M. Basieva*

SPELL: OK